Groundwater

Transient and Transition Factors in Modeling Permafrost Thaw and Groundwater Flow

by Joelle E. Langford[1], Robert A. Schincariol[2], Ranjeet M. Nagare[3], William L. Quinton[4], and Aaron A. Mohammed[5]

Abstract

Permafrost covers approximately 24% of the Northern Hemisphere, and much of it is degrading, which causes infrastructure failures and ecosystem transitions. Understanding groundwater and heat flow processes in permafrost environments is challenging due to spatially and temporarily varying hydraulic connections between water above and below the near-surface discontinuous frozen zone. To characterize the transitional period of permafrost degradation, a three-dimensional model of a permafrost plateau that includes the supra-permafrost zone and surrounding wetlands was developed. The model is based on the Scotty Creek basin in the Northwest Territories, Canada. FEFLOW groundwater flow and heat transport modeling software is used in conjunction with the piFreeze plug-in, to account for phase changes between ice and water. The Simultaneous Heat and Water (SHAW) flow model is used to calculate ground temperatures and surface water balance, which are then used as FEFLOW boundary conditions. As simulating actual permafrost evolution would require hundreds of years of climate variations over an evolving landscape, whose geomorphic features are unknown, methodologies for developing permafrost initial conditions for transient simulations were investigated. It was found that a model initialized with a transient spin-up methodology, that includes an unfrozen layer between the permafrost table and ground surface, yields better results than with steady-state permafrost initial conditions. This study also demonstrates the critical role that variations in land surface and permafrost table microtopography, along with talik development, play in permafrost degradation. Modeling permafrost dynamics will allow for the testing of remedial measures to stabilize permafrost in high value infrastructure environments.

Introduction

Approximately 24% of the land mass in the Northern Hemisphere is underlain by permafrost (Zhang et al. 2003a). Under modern day climate conditions, permafrost in many regions is degrading, which has caused a suite of hydrological changes, infrastructure failures, and ecosystem shifts. The most rapid permafrost thaw is occurring along the discontinuous-sporadic permafrost zone, which stretches across the base of the circumpolar region and occupies portions of Canada (Heginbottom et al. 1995), Alaska (Pastick et al. 2015), Scandinavia (Gisnas et al. 2017), Russia (Shiklomanov 2005), and China (Ran et al. 2012).

Permafrost thaw has many implications including changes in hydrological and ecological regimes such as increase in winter baseflow and mean annual streamflow (St. Jacques and Sauchyn 2009; Connon et al. 2014), release of stored carbon (Donnell et al. 2012), subsidence of forested permafrost plateaus, and complete alteration of cold region ecosystems (Jorgenson et al. 2001; Jorgenson and Osterkamp 2005). Groundwater flow paths and fluxes can be highly controlled by permafrost thaw (Walvoord et al. 2012). Current and projected permafrost degradation under highway embankments, and other infrastructure projects, is also a continuing problem (Batenipour et al. 2013; Flynn et al. 2016; Mu et al. 2016; Kurz et al. 2017). A warming of approximately 0.3 °C per decade of the shallow permafrost in the northern and central Mackenzie region of the Northwest Territories (NWT) has taken place since the 1980s, which is tied to an increase in the mean annual air temperature (Beilman and Robinson 2003; Smith et al. 2005). The permafrost of the discontinuous region is relatively warm and thin with temperatures often greater than −2 °C and thicknesses nearing 10 m (Burgess and Smith 2000).

[1]Department of Earth Sciences, University of Western Ontario, 1151 Richmond Street, N6A 5B7, London, ON, Canada.

[2]Corresponding author: Department of Earth Sciences, University of Western Ontario, 1151 Richmond Street, N6A 5B7, London, ON, Canada; 519 661 3732; schincar@uwo.ca

[3]ARKK Engineering, #168 2301 Premier Way, T8H 2K8 Edmonton, AB, Canada.

[4]Cold Regions Research Centre, Wilfrid Laurier University, 75 Avenue West, N2L 3C5 Waterloo, ON, Canada.

[5]Department of Geoscience, University of Calgary, 2500 University Dr. N.W., T2N 1N4 Calgary, AB, Canada.

Article impact statement: Transient unfrozen layer applied temperatures between permafrost table and ground surface improves permafrost groundwater model results.

Received October 2018, accepted May 2019.

doi: 10.1111/gwat.12903

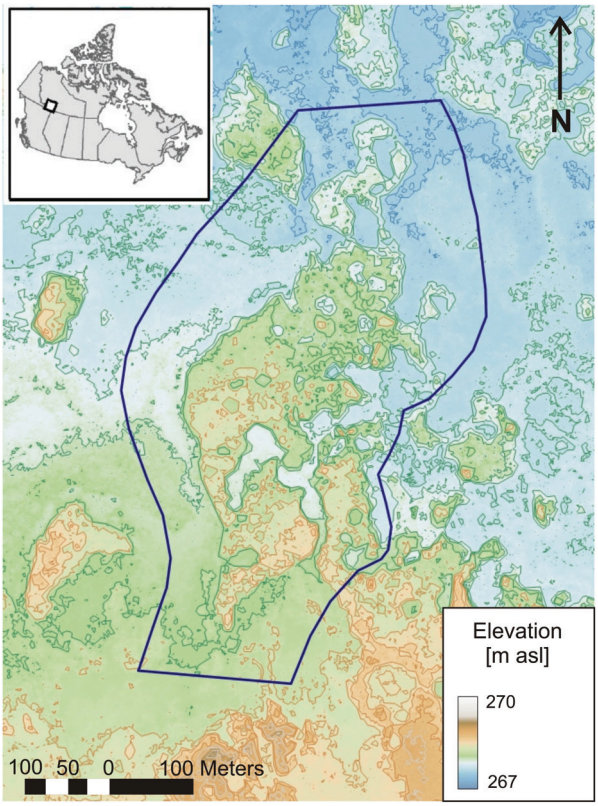

Figure 1. Aerial elevation map of the plateau-wetland complex (61°18'N, 121°18'W), outlining the study area. Inlay map shows location (square) of study site within Canada.

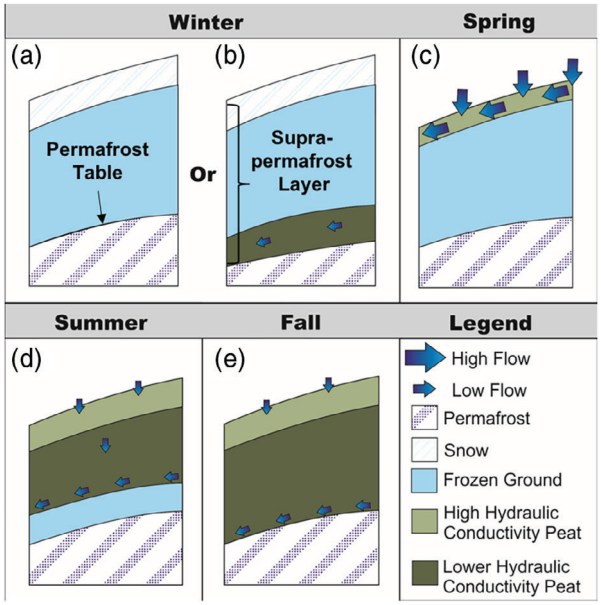

Figure 2. Conceptual figures showing subsurface flow on a permafrost plateau during (a) winter, when the freezing front extends to the permafrost table; (b) winter, when the frost table does not extend deep enough to meet the permafrost and a talik exists; (c) spring, when the ground starts to thaw and water can infiltrate and flow within the supra-permafrost zone; (d) summer, when the thaw front has extended deeper into the plateau and water can infiltrate into the relatively less porous peat; and (e) fall when the entire active layer has thawed.

Thawing ice-rich permafrost plateaus are found in the lower Liard River valley of NWT, Canada. This region is currently underlain by approximately 40% permafrost (Quinton et al. 2011) and is blanketed by an extensive layer of peat (Aylsworth and Kettles 2000). These peatlands are made up of permafrost plateaus, which are elevated approximately 1 m above the surrounding bogs and fens (Quinton et al. 2010) (Figure 1). The permafrost below the plateaus is insulated by the overlying vegetation and insulative peat. Microtopography of the permafrost table plays a critical role in the degradation of a permafrost plateau (Wright et al. 2009; Connon et al. 2018) as lateral shallow groundwater flow along the permafrost table gradient allows water to pool in microdepressions. This produces regions of increased moisture content and therefore dissimilar thermal conditions in depressions and ridges. The moisture content and distribution in peat has a large effect on the material's thermal properties, and thus on its freeze-thaw characteristics. Saturated peat has a higher thermal conductivity than dry peat; therefore, the rate of thaw is enhanced in saturated microdepressions (Wright et al. 2009). This is a positive feedback system that leads to the expansion of the depression, until the permafrost has been entirely degraded (Wright et al. 2009; Jorgenson et al. 2010). A positive feedback cycle is also induced along the edges of thawing permafrost plateaus. As the permafrost degrades and the ground subsides and becomes saturated, the trees become waterlogged and die, no longer providing thermal insulation for the plateau (Jorgenson and Osterkamp 2005; McClymont et al. 2013).

The current climate cycle is causing the thaw depth of the supra-permafrost layer to increase, resulting in degradation of permafrost (Walvoord and Kurylyk 2016). As the thaw deepens, the annual freeze may no longer reach the permafrost table during the winter, leaving an open channel of unfrozen ground called a talik (Figure 2). Taliks provide a route for year-round groundwater flow and increased thermal transport, leading to further deepening of the permafrost table (Zhang et al. 2008; Connon et al. 2018). Talik development can be conceptualized analogous to the role evolving fracture networks play in karstic systems.

Simulating groundwater flow and heat transport processes in permafrost environments is challenging due to the spatially and temporarily varying hydraulic and thermal properties of the shallow supra-permafrost zone, and the influence of permafrost geometry and thermal conditions on groundwater flow and heat transport dynamics (Bense et al. 2012; Kurylyk et al. 2016). Hemisphere-scale predictive models have been generated to assess the continued rate of permafrost degradation (Doven et al. 2013). There are also smaller scale models of one- and two-dimensions (Johansson et al. 2015; Williams et al. 2015; Gao et al. 2016; Mohammed et al. 2017; Shojae Ghias et al. 2017), and three-dimensions (Kurylyk et al. 2016; Schilling et al. 2019) used to study freeze-thaw processes and permafrost thaw on a local scale. Finally,

there are advanced three-dimensional fully coupled surface/subsurface thermal hydrology models which run in highly parallelized computational environments (Painter et al. 2016). To the best of our knowledge, a three-dimensional model of a permafrost plateau that includes the supra-permafrost zone and surrounding wetlands has not yet been developed. Such a model, as developed in this study, allows for a stronger understanding of the thermal transport processes taking place in plateau-wetland complexes. For example, a modeling approach that develops realistic talik formation is critical in the study of permafrost degradation. Braverman and Quinton (2016) found that talik conduits can convey significant quantities of groundwater throughout the year in permafrost plateaus, and provided a conceptual framework for the development of thermo-hydrological numerical models in this sensitive region. Further advancement of permafrost modeling methodologies will lead towards development of improved permafrost protection methods and permafrost thaw predictions. This will allow for the advancement of remedial methods as outlined in Mohammed et al. (2017) to field scale applications.

Study Area

The permafrost plateau being modeled is located within the Scotty Creek drainage basin, approximately 50-km south of Fort Simpson (61°18'N, 121°18'W) NWT (Figure 1). This basin is part of the sporadic-discontinuous permafrost region of Canada with an approximate distribution of 43% shallow, ice-rich permafrost peat plateaus, surrounded by fens (21%), connected and isolated bogs (27%) and lakes (9%) (Quinton et al. 2010). Geophysical studies in the region by McClymont et al. (2013) found the thickness of the permafrost plateaus in the region to range from 5 to 13 m (Figure 3).

The silty clay glacial deposits, indicated in Figure 3, are overlain by a thin silt-sand layer (Aylsworth and Kettles 2000). Above these glacial deposits is an extensive layer of organic peat which ranges in thickness from about 2 to 4 m (Aylsworth and Kettles 2000). The state of peat decomposition affects its hydraulic properties (Grover and Baldock 2013). The peat may be subcategorized into an upper layer (0-0.2 m) that has a lower bulk density and higher porosity, and is more hydraulically conductive, than the lower more decomposed layer (0.2-3 m) (Quinton et al. 2008).

The thin warm permafrost region is sustained under rising mean annual air temperatures because peat acts as thermal insulation between the atmosphere and frozen ground. The vegetation of the peat plateaus is composed of black spruce trees, as well as small shrubs, lichens and mosses, all of which insulate and sustain the permafrost in a warming climate (Quinton et al. 2010). A vegetative mat composed of sedges floats approximately 5-20 cm below the water surface of the fens (Quinton et al. 2003), moving up and down with the water level (Garon-Labrecque et al. 2015). The region has a dry continental climate, with long cold winters and short hot and

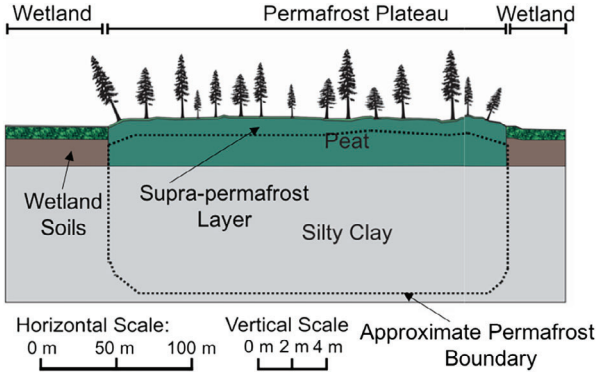

Figure 3. Cross-section of a characteristic plateau-wetland complex in Scotty Creek, NWT.

dry summers (Meteorological Service of Canada 2017). Annual evapotranspiration in the region is approximately 295 ± 43 mm/year (Warren et al. 2018). The average annual rainfall in Scotty Creek is 369 mm, of which just under half falls as snow (Meteorological Service of Canada 2017). Snow pack peaks in March then rapidly ablates and melts creating the spring freshet. Plateaus act as runoff generators in Scotty Creek and in similar basins in the discontinuous permafrost fringe (Quinton et al. 2010). Subsurface flow through the active (i.e., seasonally thawed) layer is the main runoff pathway from plateaus (Figure 2c) (Wright et al. 2008). Basin drainage from plateaus is transported through connected fens and bogs to rivers and connected lakes (Quinton et al. 2010).

Methods

The Simultaneous Heat and Water (SHAW) flow model (Flerchinger and Saxton 1989) and the model FEFLOW (DHI-WASY 2016), with the piFreeze freeze-thaw plug-in (Clausnitzer and Mirnyy 2016), were used to conduct the simulations. SHAW is a one-dimensional soil-vegetation-atmosphere-transfer modeling program that simulates the surface water and energy balance, as well as the subsurface flow of heat, water, and solutes accounting for soil freeze-thaw processes. A detailed description of SHAW can be found in Flerchinger (2000, 2017). FEFLOW is a three-dimensional saturated-unsaturated groundwater flow, heat and solute transport simulation software (DHI-WASY 2016). The piFreeze plug-in (Clausintzer et al. 2016) allows simulation of saturated-unsaturated conditions with phase change using FEFLOW. We employed the latest version of SHAW (SHAW 3.0) which includes lateral subsurface runoff, implemented as a sink term. This is an important process in highly porous media such as peat, and the dominant runoff mechanism on peat plateaus. Model calibration efforts showed including subsurface runoff was critical for accurately reproducing measured subsurface temperature and moisture regimes of the active layer. The SHAW simulation outputs, specifically ground surface temperature and net water transfer at ground surface (summation of SHAW outputs of daily infiltration, overland runoff and

evapotranspiration), were applied as the upper thermal and recharge (fluid-flux) boundary conditions for the transient FEFLOW simulations (Figure S1, Supporting Information).

Two SHAW models were developed, one to represent the permafrost plateau and one to represent the surrounding wetlands or fens. The different material properties used in the SHAW simulations can be found in Tables S1 and S2. The material properties used to develop the FEFLOW model were based on measurements and studies done at the Scotty Creek Research Station (see Table S3 and Figure S2) and work by Sjoberg et al. (2016) for the fens, and Aylsworth and Kettles (2000), Kurylyk et al. (2016), Nagare et al. (2013), and Zhang et al. (2010) for the plateau and underlying glacial till. Meteorological data for the SHAW model, including maximum and minimum air temperature, dew point temperature, precipitation, radiation, and wind run, were collected at weather stations at Scotty Creek (2005 to 2015) and Fort Simpson (Environment Canada, Fort Simpson, Northwest Territories, Canada). Meteorological data were projected back to 1875, the start of the most recent warming trend, using trend data from McClymont et al. (2013). Air temperature inputs and SHAW ground temperature outputs, for the wetland and plateau, from 1875 to 2015 can be seen in Figure S3.

FEFLOW's piFreeze plug-in modifies the Richards' equation to account for changes in porosity and liquid water content which occur when ice develops and melts (Clausnitzer and Mirnyy 2016; DHI-WASY 2016). PiFreeze also modifies FEFLOW's constitutive equations of effective thermal conductivity, and heat capacity of the media to account for ice content and the latent heat of phase change in its governing heat transport equation (Clausnitzer and Mirnyy 2016). The FEFLOW-piFreeze code has been validated against the InterFrost group test cases as outlined in Ruhaak et al. (2015) and Grenier et al. (2018). The FEFLOW flow model boundaries surrounding the plateau were based on their alignment with physical and hydraulic features that are assumed to remain stable throughout the model's projected time frame. Following previous studies (Hayashi et al. 2004; Christensen et al. 2010; Quinton et al. 2010) the eastern and western model domain boundaries were assumed to align with the direction of groundwater flow in the fen (Figure 4). The northern and southern boundaries were selected to be perpendicular to fen water flow, thus along topographic isolines, assuming water at surface (Figure 4). Surface topography was based on LIDAR imagery acquired in 2008 at a horizontal resolution of 1 m × 1 m and vertical resolution of 0.18 m.

Coupled water and heat flow models are highly sensitive to changes in water and ice content as these affect the hydraulic and thermal properties of the variably saturated zone. Thus, the importance of simulating changes in temperature, and water and ice contents, with high accuracy. Due to high thermal gradients between ice and atmosphere, or ice and groundwater, model discretization considerations were of upmost importance.

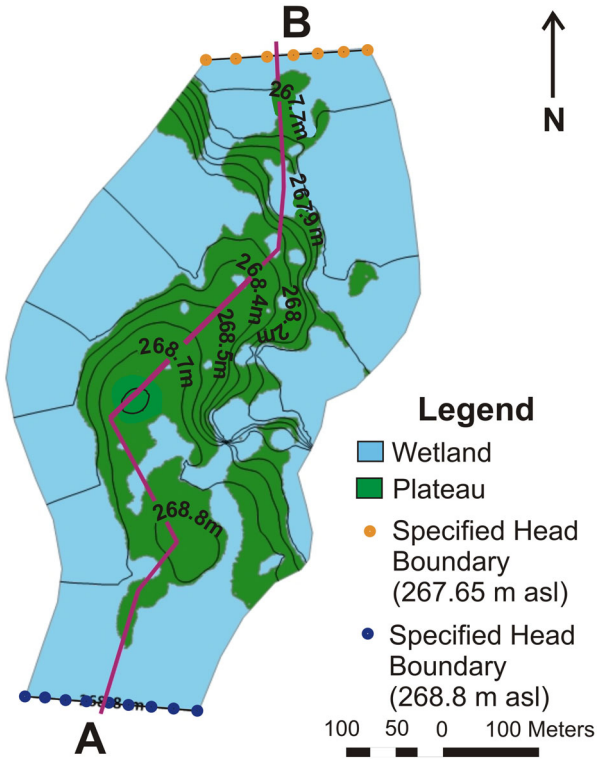

Figure 4. FEFLOW model boundary conditions, typical summer hydraulic head distribution, and location of cross-section A-B for Figure 7.

Multiple sensitivity tests on subdomain models were run to assess horizontal and vertical discretization. Nodal or layer spacing was as dense as 0.01 m in the SHAW plateau model and 0.1 m in the FEFLOW model close to the surficial thermal boundary conditions. Further information on discretization is provided in Table S4.

For the transient FEFLOW simulations, monthly averages of SHAW-derived daily ground surface temperatures (0.05-m depth for plateau and 0.1-m depth for wetland), and daily net water transfer at ground surface, were used as boundary conditions at the surface. Application depths vary as the wetland SHAW model was not as finely discretized as the plateau model. The monthly average temperature was used to decrease the computational effort, after conducting sensitivity tests using daily input. Sensitivity tests involve full-model runs over sufficient time periods to assess model fits to field data. A daily input time-step was used for water transfer, because vadose zone water content changes needed to be defined at a finer resolution to properly account for changes in thermal and hydraulic properties. Throughout the transient simulations, constant hydraulic head boundaries were applied at the northern and southern boundary (Figure 4). While the average annual range of water level fluctuation in the Scotty Creek wetlands is 0.5 m, model testing confirmed these variations had a negligible effect on the plateaus, the focus of this study. Hydraulic head distributions (Figure 4) agreed well with field based conceptual models of the permafrost plateaus as being runoff generators (Quinton and Hayashi 2005) feeding surrounding

wetlands. As confirmed by model sensitivity tests, heat transfer at the plateau—wetland scale is dominated by vertical heat conduction. Thus, a zero-gradient temperature condition was used and heat left the lateral boundaries by advection.

The flow and thermal initial conditions for the transient FEFLOW simulations, including the state of permafrost, were developed using two approaches. First a steady-state approach, similar to Kurylyk et al. (2016), was followed. In this approach, a constant ground temperature of −2.5 °C was applied over the modern-day permafrost plateau and 1.3 °C over the modern-day wetlands (Kurylyk et al. 2016). The base of the model was assigned a constant temperature of 1.5 °C following field data from Smith et al. (2005). The initial permafrost state was also developed using a transient spin-up methodology. For the transient spin-up model run, model nodes between 1 and 30 m below ground surface (mbgs) under the peat plateau were assigned an initial temperature of −1 °C. The model nodes in the upper 1 m, as well as below 30 mbgs, were assigned an initial temperature of 1.5 °C. All model nodes under the wetlands were assigned an initial temperature of 1.5 °C. A key difference between the steady-state and the transient spin-up initial condition development approaches is that in the steady-state approach permafrost development is forced from the ground surface. This freezes the supra-permafrost zone resulting in unrealistic initial conditions. However, the transient spin-up approach results in a more realistic initial condition that better matches field data.

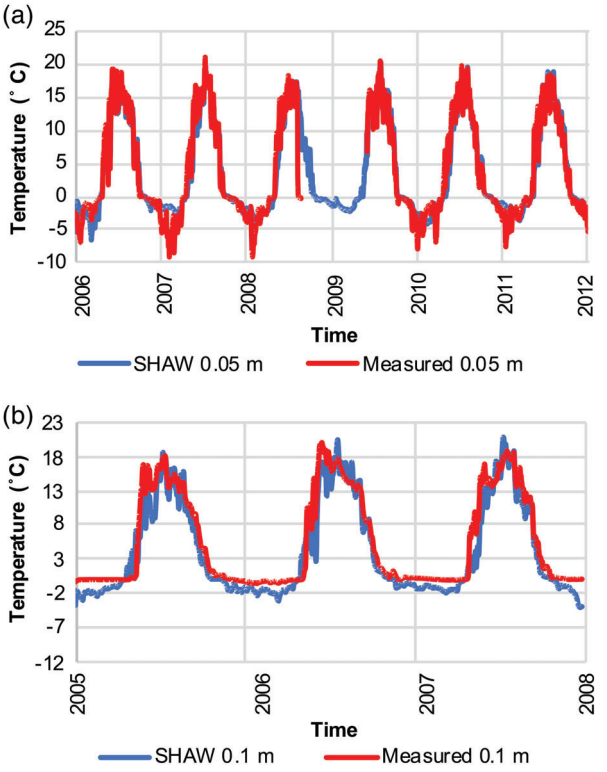

Figure 5. The observed vs. SHAW-modeled (a) plateau ground temperatures at 0.05 m, and (b) wetland ground temperatures at 0.1 m. Time period reflects available field data which varied between plateau and wetland. Note: sensor failure occurred between August 2008 and May 2009 on plateau.

Results

Model Calibrations

The SHAW models were calibrated to ground temperatures and soil moisture contents measured on the peat plateau and wetlands, as well as overall water balance for the 2006 to 2012 period. Observed and SHAW modeled temperatures, at 0.05 mbgs on the plateau and 0.1 mbgs on the wetland, are shown in Figure 5. These depths represent the input depths for the FEFLOW model. Water balance results for a typical water year can be seen in Figures S5 and S6. The SHAW peat plateau and wetland models had a mean absolute error (MAE) of 0.24 °C and 0.33 °C, and a standard error (SE) of 0.01 °C and 0.02 °C, respectively, calculated daily. The SHAW models have periods where they do not match observed temperatures as well, particularly during winter (Figure 5). Winter period mismatches can be attributed to the one-dimensional nature of the SHAW models which do not account for the significant snow redistribution that occurs over the plateau and wetland during winter. In addition, the fen freezes to a depth of approximately 1 m, and below this depth is unfrozen and relatively warm (~2 °C) slowly flowing water. This three-dimensionality is not represented in the SHAW models. Kurylyk et al. (2016) experienced similar errors early in the year with their one-dimensional NEST (Zhang et al. 2003b) model. Some of the lateral subsurface runoff in SHAW, especially during periods of short-lived surface ponding, is not explicitly transferred or represented during coupling from one-dimensions (SHAW) to three-dimensions (FEFLOW) simulations. However, as the peat surficial soils readily infiltrate water, surface ponding is a minor process only occurring at the plateau edges.

The FEFLOW model was calibrated using November 2004 to November 2006 ground temperatures at different depths. FEFLOW plateau ground temperatures compared well to the measured ground temperatures (Figure 6). The modeled temperatures lack the daily temperature spikes because the average monthly ground temperature was applied, however, trends are maintained. The MAE ranges from 0.06 °C at 0.7-m depth, to 0.23 °C at 0.1-m depth. The model was highly resolved numerically over the 0.7-m depth being discretized into 27 slices ranging from 0.01 to 0.05 m. This level of refinement was found necessary to properly represent thermal transport and avoid numerical dispersion.

Simulation Using Steady-State Initial Conditions

The initial conditions permafrost body has a rounded base with its deepest portions in the center of the plateau (Figure 7a). The 1.3 °C temperatures applied on the wetlands prevented permafrost from developing shallower than 10 m, but permafrost does underlie some

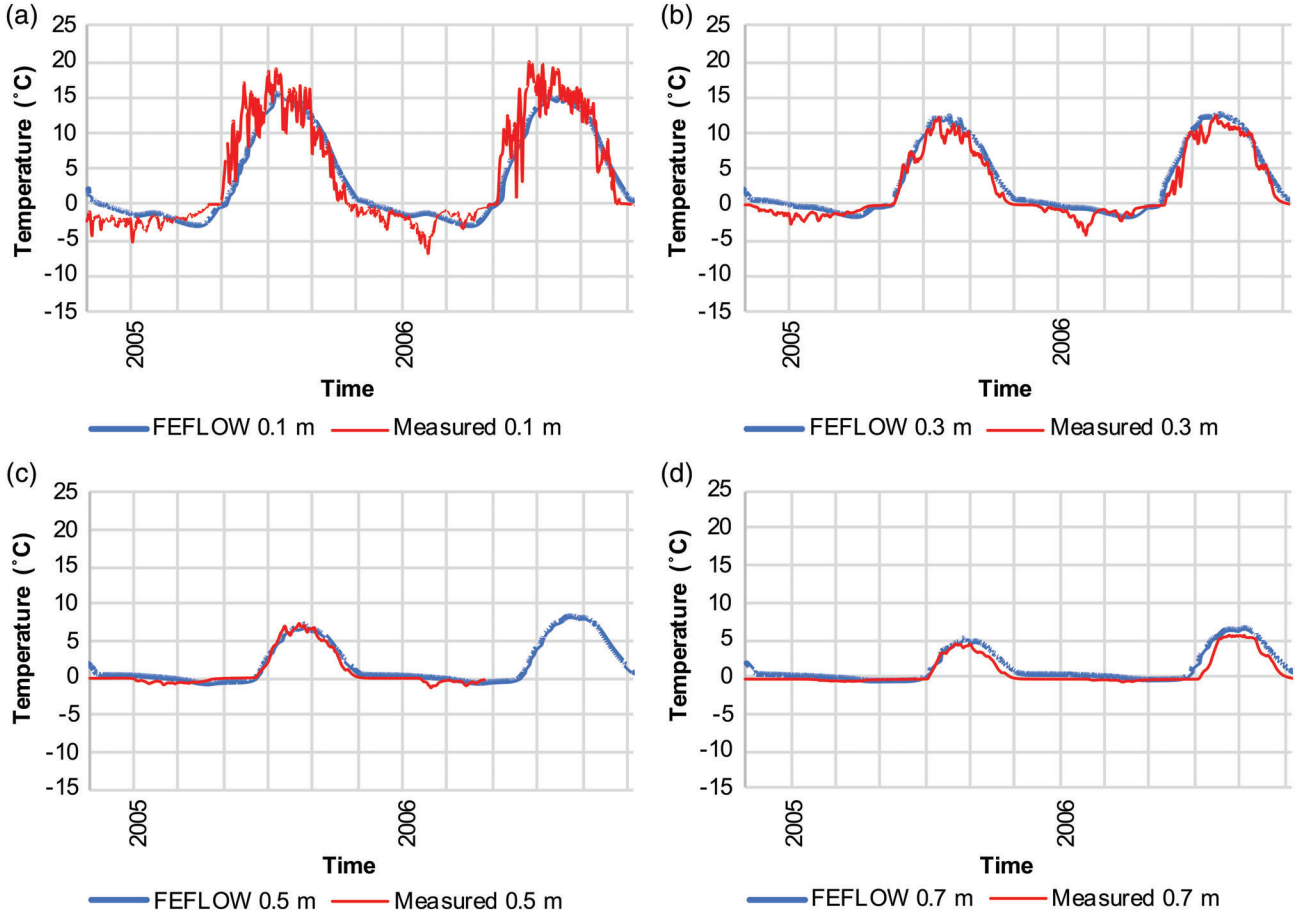

Figure 6. The observed vs. modeled plateau ground temperatures at depths (a) 0.1 m, (b) 0.3 m, (c) 0.5 m, and (d) 0.7 m from November 2004 to November 2006.

smaller wetland regions between permafrost plateaus due to adjoining adjacent bodies (Figure 7a). Model results in this area of the plateau show permafrost extending to 15 m, which compares well to the 16 m-depth measured by McClymont et al. (2013).

Transient simulations under the 1875 to 2015 climate conditions, using the initial conditions developed using the steady-state approach, had thaw rates beyond that which would correspond with the imposed climate conditions. Thus the simulations were stopped at the end of 1924. Permafrost distributions after 25 and 50 years, for the zoomed in area depicted in Figure 7a, are shown in 7b and 7c. Taliks, routes for year-round groundwater flow and increased thermal transport, are clearly evident as zones above 0 °C and between the 0 °C isotherms at surface and depth (Figure 7b and 7c). A higher rate of permafrost thaw was expected as the plateau, and thus permafrost body, was much more laterally extensive in 1875. While the oldest imagery available for the area (1947) shows the modeled region was once surrounded to a much larger degree with permafrost, topographic and permafrost data were only available for the "current" condition.

Model simulations showed that the thinnest portions of the permafrost body, the north and south points, thawed at the quickest rate. The eastern half of the permafrost plateau thawed vertically from the surface more rapidly than the western half. The western portion of the plateau has a relatively smooth higher elevation and the eastern half consists of many small depressions. Water collects in these small depressions, generating regions of higher bulk thermal conductivity than the surrounding elevated drier peat. This increased bulk thermal conductivity leads to increased vertical permafrost thaw and talik development. Permafrost with and without an overlaying talik deepened at rates of approximately 0.04 and 0.1 m/year, respectively. The horizontal thinning of the plateau from the eastern and western parts of the plateau were both approximately 0.5 m/year. This supports field observations that the eastern portion of the plateau is thawing more quickly and that it is due to vertical thermal effects and not simply from the adjoining wetlands.

Simulation Using Transient Spin-Up Initial Condition

The transient spin-up method of developing initial conditions does not create a bulbous body of permafrost as the steady-state method does. Instead, the permafrost body has equal depth below all points of the plateau, forming a linear base with defined edges (Figure 7d). The transient spin-up approach leaves an initially thawed portion of overlying ground, the supra-permafrost layer. This difference is significant because ice has a thermal conductivity over three times greater than that of water.

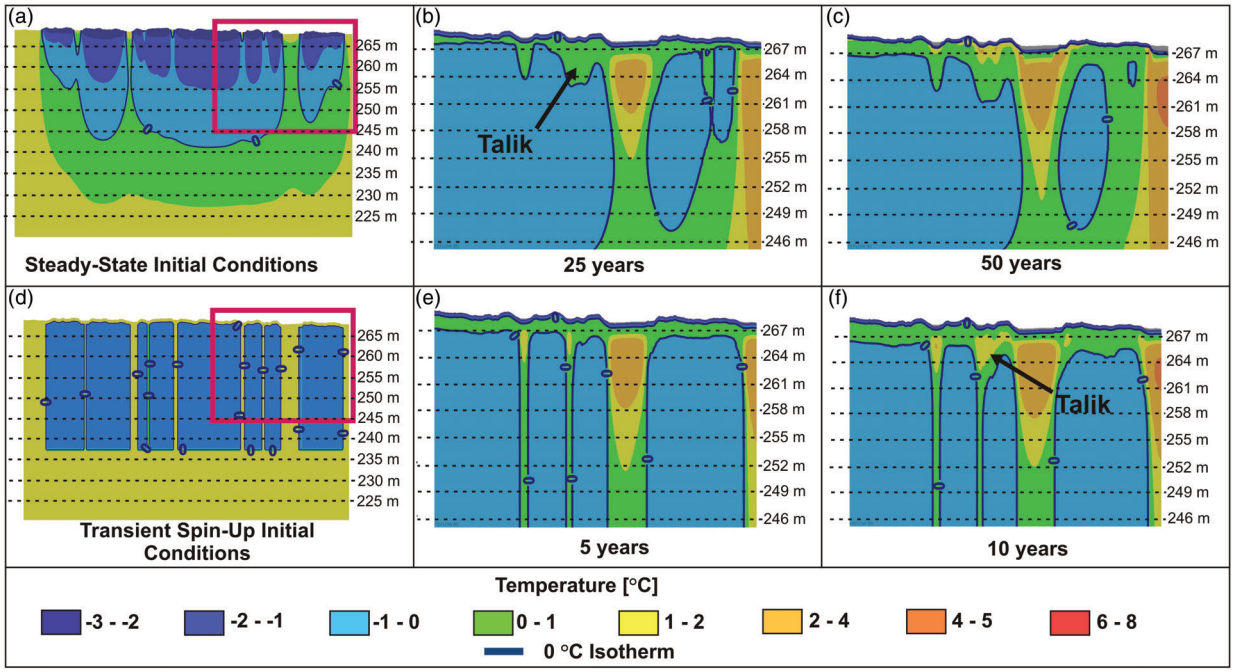

Figure 7. The progression of the permafrost thaw over time: (a) using steady-state initial conditions along transect A-B [approximately 800 m] as identified in Figure 4; (b) and (c) zoomed in area depicted by red box after 25 and 50 years using steady-state conditions; (d) using transient initial conditions along transect A-B as identified in Figure 4; (d) and (e) zoomed in area depicted by red box after 5 and 10 years using transient initial conditions.

Transient simulations under the 1999 to 2015 climate conditions, using the transient spin-up initial conditions approach, resulted in more realistic plateau thaw rates. Thaw did not propagate as deep as with the steady-state initial condition approach. Permafrost distributions after 5 and 10 years, for the zoomed in area depicted in Figure 7d, are shown in Figure 7e and 7f. Again, taliks are clearly evident as zones above 0 °C and between the 0 °C isotherms at surface and depth (Figure 7e and 7f). Groundwater velocities through the taliks are highly variable, both spatially and temporally. To demonstrate this, the groundwater flow along a talik profile in the model was studied under freezing surface conditions (December) after 10 years of model run (Figure 7f). Within a thawed peat layer at 1.7-m depth, flow was simulated to be approximately 4×10^{-7} m/s. Flow in partially frozen peat just above this was approximately 2×10^{-7} m/s. Groundwater velocities at increasingly shallower depths drop to essentially zero due to frozen ground conditions. Groundwater velocities also decrease with increasing depth due to the low permeability of the permafrost. Plateau temperature MAE ranges were 0.36 °C to 0.52 °C, which is less than half that of the steady-state initial condition model results. The two methods produced similar wetland temperature results with nearly identical MAEs, ranging from 0.46 °C at 0.1 m to 0.84 °C at 1.3-m depth. Model temperatures fit field observations very well at surface but illustrate an enhanced warming with depth during spring, while peak summer and fall trend matches are maintained (Figure 8). The enhanced warming with depth during spring is, to some extent, the result of using average monthly ground surface temperatures. This averages out diurnal cold periods in the spring and results in above 0 °C temperatures being applied to thawing ice. Near surface temperatures are not as affected as they remain fairly close to air temperatures. Submodel sensitivity analyses using hourly ground surface temperatures improved results but significantly increased computational resources. Thus the decision to use monthly ground surface temperatures was taken in order to maintain a balance between computational time and model accuracy, and the overall purpose of the model.

Discussion

The dominant form of hydrological response in permafrost plateaus, which was accurately represented in this model, is subsurface runoff within the supra-permafrost layer (Figure 2). The dominant sources of subsurface runoff are snow melt and precipitation, both of which are applied to the ground surface. It was found that the net surface water transfer could be applied in time steps no longer than daily, to properly develop supra-permafrost layer moisture conditions. Average weekly or monthly net surface water transfer does not allow the ground surface to be exposed to dry periods, which is important for permafrost insulation. Groundwater flow paths are shallow and dominantly along the permafrost table.

The supra-permafrost layer was found to be the most critical zone of heat transport in a permafrost thaw model because it is through this zone that heat is transferred

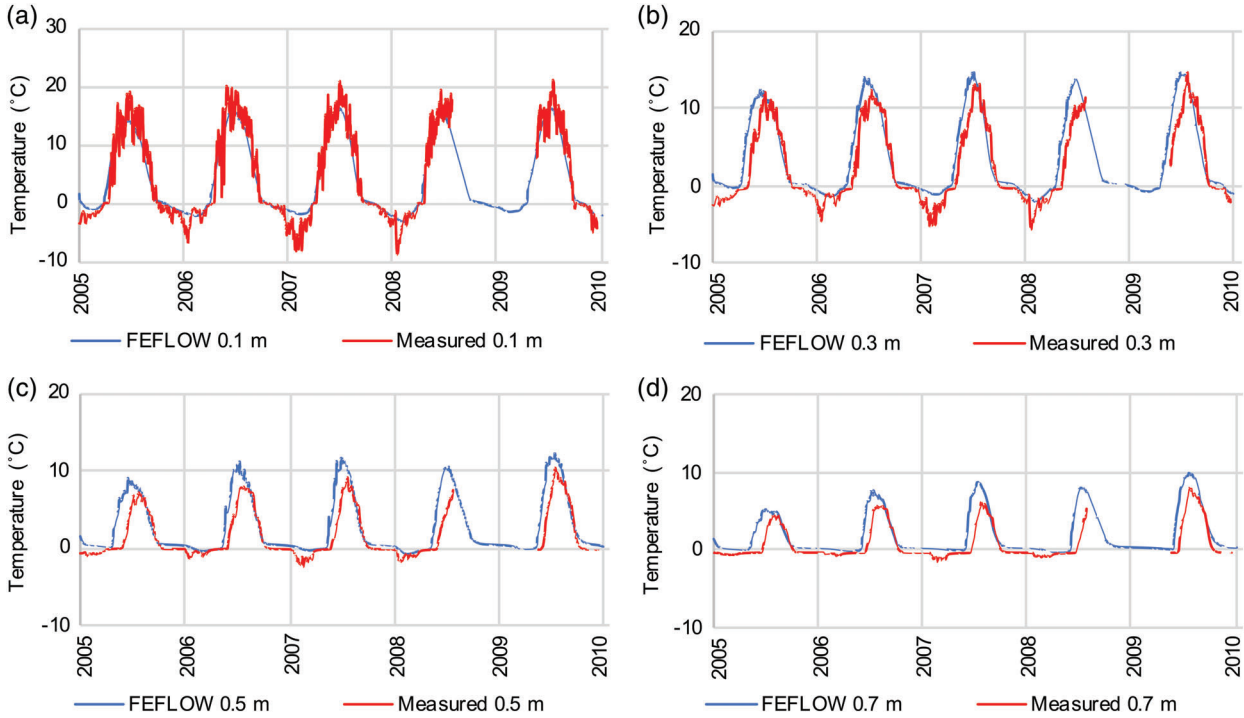

Figure 8. Plateau observed and FEFLOW modeled with transient initial condition ground temperatures with time at depths (a) 0.1 m, (b) 0.3 m, (c) 0.5 m, and (d) 0.7 m. Sensor failure occurred between August 2008 and May 2009.

between the ground surface and the permafrost. To increase the accuracy in this layer, discretization was optimized. It was found that a nodal spacing as fine as 0.01 m close to the temperature boundary condition was required for the FEFLOW model to properly compute thermal transport. The initial temperature conditions of the supra-permafrost layer proved to have a large effect on the transient ground temperature results. The initial conditions of most flow models are steady-state conditions developed from averaged boundary conditions. However, the initial conditions for thawing permafrost cannot be steady-state because the system is always transitioning, and not in equilibrium. Geomorphological and topographical conditions are constantly evolving to create an ever-expanding network of diminished peat plateaus and expanding wetlands.

A spin-up period refers to the model simulation time required to bring the steady-state conditions, or one set of transient conditions in the case of permafrost, to representative transient climate forcing. Here it was found that a spin-up period of approximately 3 years was required for an initial conditions permafrost body to develop a representative supra-permafrost layer, and possibly taliks. When permafrost is aggraded in steady state from the plateau ground surface, ice fills the pores of the shallow peat which increases the bulk thermal conductivity of the media. This increase in bulk thermal conductivity causes rapid thaw to propagate so deep into the permafrost that a talik immediately develops. As taliks provide for year round groundwater flow and thus enhanced thermal transport, this leads to increased thaw rates beyond that which would correspond with the imposed climate conditions. However, when initial conditions include a layer between the permafrost table and the ground surface that is not frozen, and simulation is conducted using time-varying surficial boundary conditions, what we deem here as using a transient spin-up method, it results in a better match of simulated thaw rates to the observed data. This layer acts as a thermal buffer of lower bulk thermal conductivity that maintains shallow permafrost throughout the spin-up period. Thermal gradients are then more accurately represented in the supra-permafrost layer. In this study an initial unfrozen layer of 1 m was applied. However, the optimal initial condition unfrozen layer will likely be different for each field site. While taliks still develop, they do so at more realistic depths and rates, thus showing the importance of properly representing groundwater flow and thermal transport.

The dominant groundwater flow is within the supra-permafrost layer, however, it is the development of groundwater conduits within the permafrost, or taliks, which play a key role in peat plateau and permafrost degradation. These conduits are spatially and temporally highly variable, and unlike karst which continually evolves to larger networks, talik networks can reduce in size, connectivity, and permeability during colder conditions.

Conclusions

A permafrost plateau-wetland complex is a dynamic thermal transport and hydrogeological flow system. Due to the low hydraulic gradient in the Scotty Creek region (~0.003 m/m), thermal flow is dominated by conduction

through water, ice and ground materials. This dynamic system has been developed over hundreds of years under shifting climate regimes and geomorphology. Accurately representing all the processes occurring in such a system through time is impossible as all the necessary historical data do not exist. However, this study determined the methods that are critical to building a transient thawing permafrost plateau model. It was found that applying appropriate initial conditions is vital to develop an accurate thermal gradient in the supra-permafrost layer, and thus accurate thermal transport from the surface boundary to the permafrost table. Model testing showed that developing a steady-state permafrost plateau from ground surface freezing temperatures yielded an inaccurate thermal gradient in the supra-permafrost layer, which lead to a more rapid permafrost thaw than observed in the field. However, the application of a transient spin-up method, which includes a layer of unfrozen ground between the top of the supra-permafrost layer and ground surface, yielded results that more closely matched field conditions. It was found that the net surface water transfer could be applied in time steps no longer than daily, to properly develop supra-permafrost layer moisture conditions. Average weekly or monthly net surface water transfer does not allow the ground surface to be exposed to dry periods, which is important for permafrost insulation.

While field observations point to the critical role permafrost table microtopography plays in the degradation of a permafrost plateau, this modeling study provided new and valuable insights into the time sequencing of this process. Simulations demonstrate how temperature, soil moisture, and groundwater flow vary with permafrost thaw and associated feedback cycles. The three-dimensional nature of permafrost thaw is clearly evident through the complex development of taliks which allow for enhanced groundwater flow and thermal transport. In many ways the importance of taliks is similar to that of evolving karst conduits in groundwater flow with permafrost being representative of the less permeable rock matrix. As permafrost table microtopography manifests from surface microtopography, the importance of high-resolution surface elevation data (i.e., LiDAR) for accurate modeling is shown to be vital.

Acknowledgments

This research was funded by the Natural Sciences and Engineering Research Council (NSERC) of Canada, and supported by the Consortium for Permafrost Ecosystems in Transition, CPET (funded by NSERC and Polar Knowledge Canada). The authors would like to thank Gerald N. Flerchinger, USDA Agricultural Research Service, for his technical guidance with SHAW. The authors also wish to thank the Dehcho First Nations, particularly the Liidlii Kue First Nation and the Jean-Marie River First Nation on whose land this research was conducted, for their support.

Authors' Note

The author(s) does not have any conflicts of interest.

Supporting Information

Additional supporting information may be found online in the Supporting Information section at the end of the article. Supporting Information is generally *not* peer reviewed.

Figure S1. A flow chart demonstrating the data flow from initial climate data to the FEFLOW model.
Figure S2. Cross-section display of FEFLOW model properties. K = hydraulic conductivity with component directions.
Figure S3. Air temperature inputs and SHAW ground temperature outputs for the wetland and plateau for 1875 to 2015. Following McClymont et al. 2013 a trend of 0.015 °C/year was applied to the 1900 to 1910 average air temperature to estimate air temperatures between 1875 and 1900.
Figure S4. A cross-section showing the vertical discretization of the FEFLOW model.
Figure S5. The SHAW plateau daily water balance output of 2010 (a typical water year). The 2010 annual total of precipitation is 585.4 mm, evapotranspiration is 50.5 mm and runoff is 129.6 mm.
Figure S6. The net surface water transfer from the SHAW output water balance of 2010 (a typical water year). The 2010 cumulative net water transfer is 537 mm/year.
Table S1. SHAW model plateau properties.
Table S2. SHAW model wetland properties.
Table S3. FEFLOW model properties. Superscripts denote the term sources, equate 'a' to Kurylyk et al. 2016; 'b' to McClymont et al. 2013 and 'c' to Zhang et al. 2010.
Table S4. Vertical discretization of FEFLOW model.

References

Aylsworth, J.M., and I.M. Kettles. 2000. Distribution of peatlands. In *The Physical Environment of the Mackenzie Valley, Northwest Territories: A Base Line for Assessment of Environmental Change*, Vol. 547, ed. L.D. Dyke, and G.R. Brooks, 49–55. Ottawa, Canada: Geological Survey of Canada Bulletin.

Batenipour, H., M. Alfaro, D. Kurz, and J. Graham. 2013. Deformations and ground temperatures at aroad embankment in northern Canada. *Canadian Geotechnical Journal* 51: 260–271.

Beilman, D.W., and S.D. Robinson. 2003. Peatland permafrost thaw and landform type along a climate gradient. In *Proceedings Eighth International Conference on Permafrost*, Vol. 1, ed. M. Phillips, S.M. Springman, and L.U. Arenson, 61–65. Zurich, Switzerland: A.A. Balkema.

Bense, V.F., H. Kooi, G. Ferguson, and T. Read. 2012. Permafrost degradation as a control on hydrogeological regime shifts in a warming climate. *Journal of Geophysical Research* 117: F03036. https://doi.org/10.1029/2011JF002143

Braverman, M., and W.L. Quinton. 2016. Hydrological impacts of seismic lines in the wetland-dominated zone of thawing, discontinuous permafrost, Northwest Territories, Canada. *Hydrological Processes* 30: 2617–2627. https://doi.org/10.1002/hyp.10695

Burgess, M.M., and S.L. Smith. 2000. Shallow ground temperatures. In *The Physical Environment of the Mackenzie Valley, Northwest Territories: A Base Line for the Assessment of Environmental Change*, ed. L.D. Dyke and G.R. Brooks, 89–103. Ottawa, Canada: Geological Survey of Canada.

Christensen, B., Hayashi, M., and Quinton, W.L. 2010. Hydrology of discontinuous permafrost: Effects of permafrost plateau geometry on subsurface drainage. Paper presented at 63rd Canadian Geotechnical Conference and 6th Canadian Permafrost Conference, Calgary, AB, Canada. pp. 1259–1264.

Clausnitzer, V., and V. Mirnyy. 2016. Modeling groundwater and heat flow subject to freezing and thawing. In *Mining Meets Water—Conflicts and Solutions*, 1150–1153. Leipzig, Germany: International Mine Water Association.

Connon, R., É. Devoie, M. Hayashi, T. Veness, and W. Quinton. 2018. The influence of shallow taliks on permafrost thaw and active layer dynamics in subarctic Canada. *Journal of Geophysical Research: Earth Surface* 123: 281–297. https://doi.org/10.1002/2017JF004469

Connon, R.F., W.L. Quinton, J.R. Craig, and M. Hayashi. 2014. Changing hydrologic connectivity due to permafrost thaw in the lower Liard River valley, NWT, Canada. *Hydrological Processes* 28, no. 14: 4163–4178. https://doi.org/10.1002/hyp.10206

DHI-WASY. 2016. *piFreeze, A Freeze/Thaw Plug-in for FEFLOW, User Guide, DHI-WASY GmbH*. Berlin, Germany: DHI-WASY.

Donnell, J.A.O., M.T. Jorgenson, J.W. Harden, A.D. McGuire, M.Z. Kanevskiy, and K.P. Wickland. 2012. The effects of permafrost thaw on soil hydrologic, thermal, and carbon dynamics in an Alaskan Peatland. *Ecosystems* 15: 213–229. https://doi.org/10.1007/s10021-011-9504-0

Doven, C.D., Riley, W.J., and Stern, A. 2013. Analysis of permafrost thermal dynamics and response to climate change in the CMIP5 earth system models. *Journal of Climate, American Meteorological Society* 26: 1877–1900. https://doi.org/10.1175/JCLI-D-12-00228.1

Flerchinger, G.N. 2017. *The Simultaneous Heat and Water (SHAW) Model: Technical Documentation*. Boise, Idaho: United States Department of Agriculture, Agricultural Research Service.

Flerchinger, G.N. 2000. *The Simultaneous Heat and Water (SHAW) Model: User' s Manual*. Boise, Idaho: United States Department of Agriculture, Agricultural Research Service.

Flynn, D., D. Kurz, M. Alfaro, J. Graham, and U. Arenson. 2016. Forecasting ground temperatures under a highway embankment on degrading permfrost. *Journal of Cold Regions Engineering* 30, no. 4: 04016002(1–04016002(20.

Gao, J., Z. Xie, A. Wang, and Z. Luo. 2016. Numerical simulation based on two-directional freeze and thaw algorithm for thermal diffusion model. *Applied Mathematics and Mechanics* 37, no. 11: 1467–1478. https://doi.org/10.1007/s10483-016-2106-8

Garon-Labrecque, M.E., E. Leveille-Bourret, K. Higgins, and O. Sonnentag. 2015. Additions to the boreal flora of the Northwest Territories with a preliminary vascular flora of Scotty creek. *The Canadian Field-Naturalist* 129, no. 4: 349–367.

Gisnas, K., B. Etzelmüller, C. Lussana, J. Hjort, B.K. Sannel, K. Isaksen, S. Westermann, P. Kuhry, H.H. Christiansen, A. Frampton, and J. Åkerman. 2017. Permafrost map for Norway, Sweden and Finland. *Permafrost and Periglacial Processes* 28: 359–378. https://doi.org/10.1002/ppp.1922

Grenier, C., H. Anbergen, V. Bense, Q. Chanzy, E. Coon, N. Collier, F. Costard, M. Ferry, A. Frampton, J. Frederick, J. Goncalves, J. Holmen, A. Jost, S. Kokh, B. Kurylyk, J. McKenzie, J. Molson, E. Mouche, L. Orgogozo, R. Pannetier, A. Riviere, N. Roux, W. Ruhaak, J. Scheidegger, J. Selroos, R. Therrien, P. Vidstrand, and C. Voss. 2018. Groundwater flow and heat transport for systems undergoing freeze-thaw: Intercomparison of numerical simulators for 2D test cases. *Advances in Water Resources* 114: 196–218. https://doi.org/10.1016/j.advwatres.2018.02.001

Grover, S.P.P., and J.A. Baldock. 2013. The link between peat hydrology and decomposition: Beyond von post. *Journal of Hydrology* 479: 130–138. https://doi.org/10.1016/j.jhydrol.2012.11.049

Hayashi, M., W.L. Quinton, A. Pietroniro, and J.J. Gibson. 2004. Hydrologic functions of wetlands in a discontinuous permafrost basin indicated by isotopic and chemical signatures. *Journal of Hydrology* 296, no. 1–4: 81–97. https://doi.org/10.1016/j.jhydrol.2004.03.020

Heginbottom, J.A., M.A. Dubrevil, and P.T. Harker. 1995. Canada permafrost. In *National Atlas of Canada*, 5th ed. Ottawa, Canada: Natural Resources Canada.

Johansson, E., L.G. Gustafsson, S. Berglund, T. Lindborg, J. Selroos, L.C. Liljedahl, and G. Destouni. 2015. Data evaluation and numerical modeling of hydrological interactions between active layer, lake and talik in a permafrost catchment, Western Greenland. *Journal of Hydrology* 527: 688–703. https://doi.org/10.1016/j.jhydrol.2015.05.026

Jorgenson, M.T., V. Romanovsky, J. Harden, Y. Shur, J. O'Donnell, E.A. Schuur, M. Kanevskiy, and S. Marchenko. 2010. Resilience and vulnerability of permafrost to climate change. *Canadian Journal of Forest Research* 40, no. 7: 1219–1236. https://doi.org/10.1139/X10-061

Jorgenson, M.T., and T.E. Osterkamp. 2005. Response of boreal ecosystems to varying modes of permafrost degradation. *Canadian Journal of Forest Research* 35: 2100–2111. https://doi.org/10.1139/X05-153

Jorgenson, M.T., C.H. Racine, J.C. Walters, and T.E. Osterkamp. 2001. Permafrost degradation and ecological changes associated with a warming climate in Central Alaska. *Climatic Change* 48, no. 4: 551–579. https://doi.org/10.1023/A:1005667424292

Kurylyk, B.L., M. Hayashi, W.L. Quinton, J.M. McKenzie, and C.I. Voss. 2016. Influence of vertical and lateral heat transfer on permafrost thaw, peatland landscape transition, and groundwater flow. *Water Resources Research* 52, no. 2: 1286–1305. https://doi.org/10.1002/2015WR018057

Kurz, D., M. Alfaro, and J. Graham. 2017. Thermal conductivities of frozen and unfrozen soils at three project sites in northern Manitoba. *Cold Regions Science and Technology* 140: 30–38.

Meteorological Service of Canada. 2017. *National climate data archive of Canada*. Dorval, Quebec, Canada: Environment Canada.

McClymont, A.F., M. Hayashi, L.R. Bentley, and B.S. Christensen. 2013. Geophysical imaging and thermal modeling of subsurface morphology and thaw evolution of discontinuous permafrost. *Journal of Geophysical Research: Earth Surface* 118, no. 3: 1826–1837. https://doi.org/10.1002/jgrf.20114

Mohammed, A., R.A. Schincariol, W.L. Quinton, R.M. Nagare, and G.L. Flerchinger. 2017. On the use of mulching to mitigate permafrost thaw due to linear disturbances in subarctic peatlands. *Ecological Engineering* 102: 207–223. https://doi.org/10.1016/j.ecoleng.2017.02.020

Mu, Y., G. Li, Q. Yu, W. Ma, D. Wang, and F. Wang. 2016. Numerical study of long-term cooling effects of thermosyphons around tower footings in permafrost regions along the Qinghai-Tibet power transmission line. *Cold Regions Science and Technology* 121: 237–249.

Nagare, R.M., R.A. Schincariol, A.A. Mohammed, W.L. Quinton, and M. Hayashi. 2013. Measuring saturated hydraulic conductivity and anisotropy of peat by a modified split-container method. *Hydrogeology Journal* 21, no. 2: 515–520. https://doi.org/10.1007/s10040-012-0930-7

Painter, S.L., E.T. Coon, A.L. Atchley, M. Berndt, R. Garimella, J.D. Moulton, D. Svyatskiy, and C.J. Wilson. 2016. Integrated surface/subsurface permafrost thermal hydrology: Model formulation and proof-of-concept simuations. *Water Resources Research* 52: 6062–6077. https://doi.org/10.1002/2015WR018427

Pastick, N.J., M.T. Jorgenson, B.K. Wylie, S.J. Nield, K.D. Johnson, and A.O. Finley. 2015. Distribution of near-surface permafrost in Alaska: Estimates of present and future conditions. *Remote Sensing of Environment* 168: 301–315.

Quinton, W.L., M. Hayashi, and L.E. Chasmer. 2011. Permafrost-thaw-induced land-cover change in the Canadian subarctic: Implications for water resources. *Hydrological Processes* 25: 152–158. https://doi.org/10.1002/hyp.7894

Quinton, W.L., M. Hayashi, and L.E. Chasmer. 2010. Peatland hydrology of discontinuous permafrost in the Northwest Territories: Overview and synthesis. *Canadian Water Resources Journal* 34: 311–328.

Quinton, W.L., M. Hayashi, and S.K. Carey. 2008. Peat hydraulic conductivity in cold regions and its relation to pore size and geometry. *Hydrological Processes* 22: 2829–2837. https://doi.org/10.1002/hyp

Quinton, W.L., and M. Hayashi. 2005. The flow and storage of water in the wetland-dominated Central Mackenzie River basin: Recent advances and future directions. In *Prediction in Ungauged Basisns: Approaches for Canada's Cold Regions*, 45–66. Cambridge, ON: Canadian Water Resources Association.

Quinton, W.L., M. Hayashi, and A. Pietroniro. 2003. Connectivity and storage functions of channel fens and flat bogs in northern basins. *Hydrological Processes* 17, no. 18: 3665–3684. https://doi.org/10.1002/hyp.1369

Ran, Y., X. Li, G. Cheng, T. Zhang, Q. Wu, H. Jin, and R. Jin. 2012. Distribution of permafrost in China: An overview of existing permafrost maps. *Permafrost and Periglacial Processes* 23: 322–333. https://doi.org/10.1002/ppp.1756

Ruhaak, W., H. Anbergen, C. Grenier, J. McKenzie, B.L. Kurylyk, J. Molson, N. Roux, and I. Sass. 2015. Benchmarking numerical freeze/thaw models. *Energy Procedia* 76: 301–310.

Schilling, O.S., Y.J. Park, R. Therrien, and R.M. Nagare. 2019. Integrated surface and subsurface hydrological modeling with snowmelt and pore water freeze-thaw. *Groundwater* 57, no. 1: 63–74. https://doi.org/10.1111/gwat.12841

Shiklomanov, N.I. 2005. From exploration to systematic investigation: Development of geocryology in 19th and early 20th century Russia. *Physical Geography* 26, no. 4: 249–263.

Shojae Ghias, M., R. Therrien, J. Molson, and J.M. Lemieux. 2017. Controls on permafrost thaw in a coupled groundwater-flow and heat-transport system: Iqaluit Airport, Nunavut, Canada. *Hydrogeology Journal* 25: 657–673. https://doi.org/10.1007/s10040-016-1515-7

Sjoberg, Y., E. Coon, A.B.K. Sannel, R. Pannetier, D. Harp, A. Frampton, S.L. Painter, and S.W. Lyon. 2016. Thermal effects of groundwater flow through subarctic fens: A case study based on field observations and numerical modeling. *Water Resources Research* 52: 1–16. https://doi.org/10.1002/2015WR017571

Smith, S.L., M.M. Burgess, D. Riseborough, and F.M. Nixon. 2005. Recent trends from Canadian permafrost thermal monitoring network sites. *Permafrost and Periglacial Processes* 16: 19–30. https://doi.org/10.1002/ppp.511

St. Jacques, J.M., and D.J. Sauchyn. 2009. Increasing winter baseflow and mean annual streamflow from possible permafrost thawing in the Northwest Territories, Canada. *Geophysical Research Letters* 36: L01401. https://doi.org/10.1029/2008GL035822

Walvoord, M.A., and B.L. Kurylyk. 2016. Hydrologic impacts of thawing permafrost—A review. *Vadose Zone Journal* 15, no. 6: 1–20. https://doi.org/10.2136/vzj2016.01.0010

Walvoord, M.A., C.I. Voss, and T.P. Wellman. 2012. Influence of permafrost distribution on groundwater flow in the context of climate-driven permafrost thaw: Example from Yukon Flats Basin, Alaska, United States. *Water Resources Research* 48: W07524m. https://doi.org/10.1029/2011WR011595

Warren, R.K., C. Pappas, M. Helbig, L.E. Chasmer, A.A. Berg, J.L. Baltzer, W.L. Quinton, and O. Sonnentag. 2018. Minor contribution of overstory transpiration to landscape evapotranspiration in boreal permafrost peatlands. *Ecohydrology* 11, no. 5: 1–10. https://doi.org/10.1002/eco.1975

Williams, T.J., J.W. Pomeroy, J.R. Janowicz, S.K. Carey, K. Rasouli, and W.L. Quinton. 2015. A radiative-conductive-convective approach to calculate thaw season ground surface temperatures for modelling frost table dynamics. *Hydrological Processes* 29, no. 18: 3954–3965. https://doi.org/10.1002/hyp.10573

Wright, N., M. Hayashi, and W.L. Quinton. 2009. Spatial and temporal variations in active layer thawing and their implication on runoff generation in peat-covered permafrost terrain. *Water Resources Research* 45, no. 5: 1–13. https://doi.org/10.1029/2008WR006880

Zhang, Y., S.K. Carey, W.L. Quinton, J.R. Janowicz, J.W. Pomeroy, and G.N. Flerchinger. 2010. Comparison of algorithms and parameterisations for infiltration into organic-covered permafrost soils. *Hydrology and Earth System Sciences* 14, no. 5: 729–750. https://doi.org/10.5194/hess-14-729-2010

Zhang, Y., W. Chen, and D.W. Riseborough. 2008. Disequilibrium response of permafrost thaw to climate warming in Canada over 1850-2100. *Geophysical Research Letters* 35, no. 2: 2–5. https://doi.org/10.1029/2007GL032117

Zhang, T., R.G. Barry, K. Knowles, F. Ling, and R.L. Armstrong. 2003a. Distribution of seasonally and perennially frozen ground in the Northern Hemisphere. *Permafrost*: 1289–1294.

Zhang, Y., W. Chen, and J. Cihlar. 2003b. A process-based model for quantifying the impact of climate change on permafrost thermal regimes. *Journal of Geophysical Research* 108, no. D22: 4695. https://doi.org/10.1029/2002JD003354